



AEROMAGNETIC AND RESISTIVITY TOMOGRAPHY TECHNIQUE FOR INVESTIGATING LEAKAGE PATHS IN APODU DAM, ILORIN SHEET 201, SOUTHWESTERN NIGERIA

*¹Olawumi, H.B., ²Olatunji, S., ¹Jimoh, A. and ²Abubakar, H. O.

¹Department of Geology and Mineral Science, Kwara State University, Malete, Nigeria

²Department of Geophysics, University of Ilorin, Ilorin, Nigeria

ARTICLE INFO

Article history:

Received: December 11, 2021

Revised: December 30, 2021

Accepted: December 31, 2021

Published online: December 31, 2021

Citation:

Olawumi, H.B., Olatunji, S., Jimoh, A. and Abubakar, H. O. (2021). Aeromagnetic and Resistivity Tomography Technique for Investigating Leakage Paths in Apodu Dam, Ilorin Sheet 201, Southwestern Nigeria. *The Nexus (Science Edition)*. 1(1): 24 - 29

*Corresponding Author:

Olawumi, H. B.

Department of Geology and Mineral Science, Kwara State University, Malete, Nigeria

*e-mail: olawumibolaji@gmail.com

ABSTRACT

The aeromagnetic and electrical resistivity tomography technique was used to evaluate the foundation conditions and stability of the Apodu earth dam located around Malete, Ilorin Sheet 201, Southwestern Nigeria. The Aeromagnetic data set was interpreted to identify dykes, lineaments, and magnetic sources controlling subsurface geology. The extracted lineament structures were employed to examine features controlling the distribution of surface and subsurface hydraulic substances cum stability of dam slope. Magnetic lineaments' length and parallelism in some areas suggested installation under a tensional stress field along pre-existing zones of weakness. Magnetic susceptibilities are not uniform in the area and were categorized viz: high, moderate, and low. The magnetic intensity range at Apodu dam is -644.19 to 285.40 nT. The northeastern part of the study area where the Apodu dam is located shows little or no sign of faulting and appears to be more stable structurally. Characterization of the Apodu dam subsurface for seepage appraisal using electrical resistivity tomography technique revealed that the dam is well compacted at the surface but with observed low resistivity values indicative of possible occurrences of weakness zones that are water-bearing in some areas of the dam embankment body at depths of around 8m and 25m. These observed low resistivity zones indicating a water-bearing weakness zone were connected in RTM1 and RTM2, and a possible water pathway was established. This water pathway is indicative of a possible seepage pathway and adequate measures are expected to be made to arrest the situation. In conclusion, Apodu dam is situated in a geologically stable environment as deduced from the aeromagnetic study but its earth embankment is suspected to possess areas with possible seepages zones as obtained from the electrical resistivity techniques of investigations. There is therefore a need to quickly remedy the dam earth embankment to ensure the longevity of the dam and avert possible failure.

Keywords: Aeromagnetic, Resistivity tomography, Geologic structure, Dam Seepage

INTRODUCTION

Previous experiences of dam construction in Nigeria and the world over show that many of the dams have defects related to several factors, among which are geological and geotechnical problems, for example, Cham dam in Gombe State, Gusau dam in Zamfara State, Challawa dam in Kano State, Ojirami dam in Edo State and others. This dam failure is attributed largely to poor investigations (geological and geotechnical) before the design and construction of the dams and improper maintenance and monitoring of the dams after construction. This trend needs to be checked and possibly reversed hence the need for this research to avert future occurrences of dam failures. It is important to scrutinize any proposed dam site for geologic, Structural, topographical, geotechnical, and hydrologic characteristics because these will determine to a large extent

the success or failure of such a dam. The selection of sites for the construction of structures like a dam is based on a combination of topographic, geologic, structural, geotechnical, and economic factors (Ako, 1976).

Dam structures must have a low tolerance for water seepage and must be designed to fit the site conditions in order to reduce losses (Ajayi *et al.*, 2005). Failure to address any of these could lead to seepage and, as a result, ultimate collapse of the structure (Olorunfemi *et al.*, 2000a, b). Biswas and Chartergee (1971) investigated the causes of dam failures around the world and discovered that structural and foundation issues related to piping, seepage, inadequate seepage cut-off, faults, settlements, and landslides accounted for 25% of the failures. The Aeromagnetic surveying is the determination of the variation in the geomagnetic field that occurs as a result of changes in the percentage of magnetite in

the rock. This reflects differences in the distribution and types of magnetic minerals in rocks, whether subsurface or surface. Because of the small contribution of detrital remnant magnetism, sedimentary formations do not usually have notable magnetic characteristics, but igneous and metamorphic rocks have greater fluctuations and can be used to investigate bedrock geology (Jayeoba and Odumade, 2015). Dam failure has not just economic effects, but also has a negative impact on the environment and the worth of life. Furthermore, residents are at risk in areas downstream of major dams (Leulalem *et al.*, 2016). Dam failure can be caused by structural flaws, neglect, aging, differential settlement, seepage, overtopping, and rockslides. Dam failures are uncommon, but when they do happen, they can cause significant damage and loss of life (Ezugwu, 2013). Available records also indicate that some dams are constructed with little or no foundation investigations before construction. To address these issues, geological and geotechnical investigations of a dam site chosen for detailed study are focused on identifying geological structures e.g., faulting, foliation and groundwater conditions, and erosion at the dam foundation and reservoir region, including the abutments. This would provide valuable information on the condition of such dams which will assist in taking quick safety decisions, determining appropriate mitigation methods, and also protecting the dam investments.

1.1 Study Area

The study area is located within the basement complex region of southwestern Nigeria. The dam investigated is Apodu located in Maleta town, Kwara State, Nigeria. The study area (Figure 1) falls within the coordinate that follows; 8° 45' 38.08" N, 4° 27' 28.98" E and 8°45' 28.96" N, 4°27'42.96" E. The study area is fairly accessible by footpath, minor and major road especially Ilorin-Shao-Maleta road. Accessibility to the different sample locations was possible through footpaths and un-tarred roads, some of which were newly created.

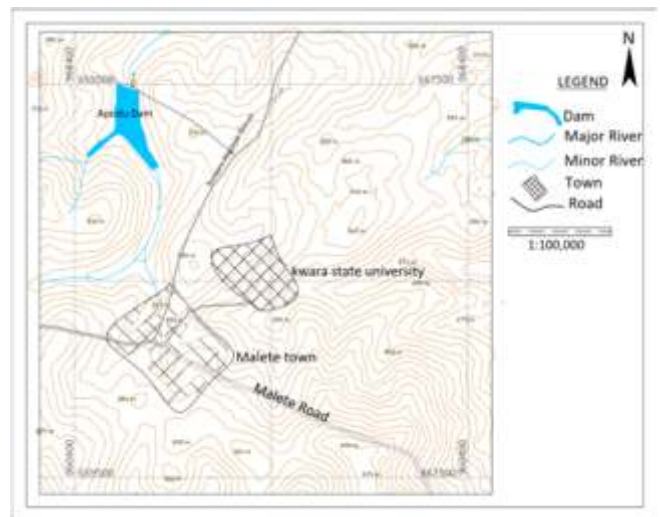
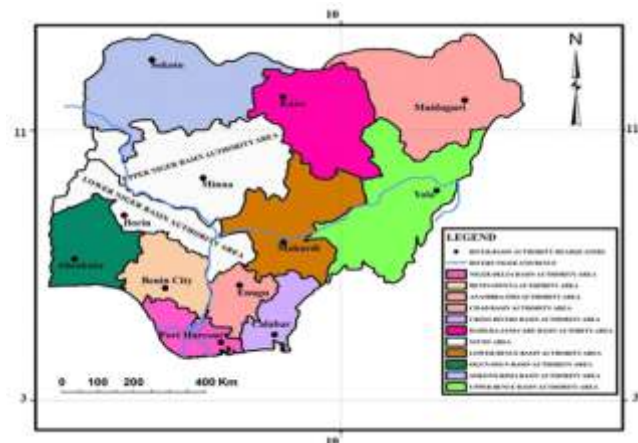


Fig 1: Location of Apodu dam

1.2 Geological Setting

The study area falls within the basement complex of southwestern Nigeria and is Archean to early Proterozoic in age. It is within the Migmatite-gneiss Complex of the Nigeria basement complex which is generally considered as the basement complex *sensu stricto* (Rahaman, 1998; Dada, 2006) because of its widespread occurrence in the Nigerian basement terrain.

Lithologies identified from the geologic map of the study area (Figure 2) include; migmatite-gneiss, porphyritic granite, and quartz veins.

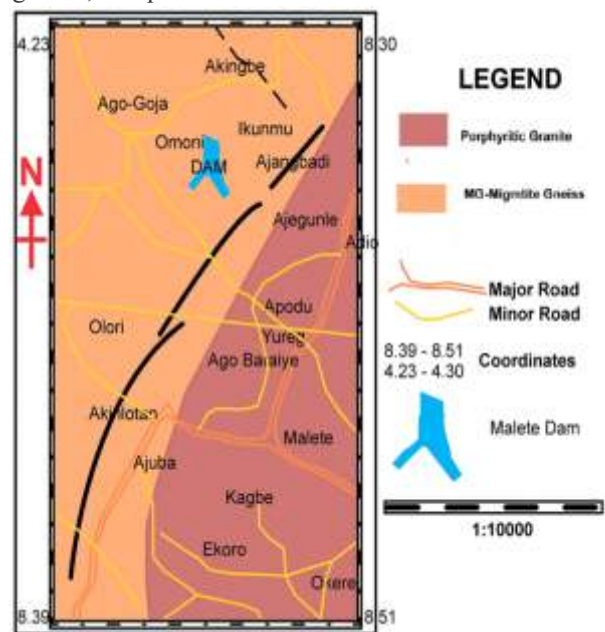


Fig 2: Updated Geological map of Apodu dam area (Modified after NGSA, 2017)

2.0 Materials and Methods

High-resolution aeromagnetic data acquired using Scintrex CS3 Cesium Vapour Magnetometer and processed by Fugro Airborne was obtained from the Nigeria Geological Survey

Agency in 2019 (MMSD, 2019). The data were systematically obtained using a Scintrex CS3 Cesium Vapor magnetometer, which is highly sensitive and measures in the range of pT (1 pT = 0.001 nT) in a 1 Hz measuring bandwidth, with sensitivity that does not decline when the detected ambient field drops. It has a range of 15,000 nT to 100,000 nT. Fixed-wing (Cessna) aircraft conducted the aeromagnetic survey, which covered a total of 235,000 line kilometers with a flight spacing of 200 meters and terrain clearance of 80 meters. The flight direction was NW-SE (135) with a flight-line spacing of 200 meters and a tie-line direction of NE-SW (45).

A recording interval of 0.1 secs and a grid mesh size of 50 meters were applied in the World Geodetic System of 1984 (WGS84) within UTM Zone 36S and with the Clark 1880/Arc 1960 coordinate system. The aeromagnetic data were processed using ENVI 5.1 image processing and analysis software. The removal of the International Geomagnetic Reference Field (IGRF) over the area improved the processed airborne magnetic field intensity. This was eventually used in the production of an aeromagnetic map. The aeromagnetic intensity data set of the area around Apodu dam (Sheet 223) was processed using Geosoft Oasis Montaj™ version 6.4.2 (HJ) software.

Surfer TM Version 12 and ArcGIS version 10.2 were also utilized for data analysis and integration, The aeromagnetic data set was upward continued to a height of about 100 m to remove near-surface noise and enhance the magnetic anomalies over the study area. Reduction to Equator (RTE), decidualization, Total Horizontal derivative, and Euler Deconvolution are some of the other data augmentation techniques used, as well as adding several structural indices to the magnetic anomaly map. The RTE was used to eliminate the magnetic inclination effect that is common in low-latitude areas. To eliminate the effect of deep-seated sources, residualization was used. To estimate the depth to the magnetic basement, a spectral analysis using the Fast Fourier Transform (FFT) method was used (DMB). The Source Edge Detection (SED) function was used to locate edges, i.e. geological contacts or peaks from potential field data by analyzing the local gradients. SED was used to estimate the location of abrupt lateral changes in magnetization and identify maxima on a grid of horizontal gradient magnitudes using the technique of Cordell and Grauch (1982, 1987).

Electrical resistivity measurements are associated with varying depths depending on the separation of the current and potential electrodes in the survey and can be interpreted in terms of a lithologic and/or geo-hydrologic model of the subsurface (Keany, 1984). The measure of resistivity (inverse of conductivity) is, sometimes, a measure of water saturation and connectivity of pore space. When it comes to filling voids, air, which has a high inherent resistance, has the opposite effect as water. Whereas water reduces subsurface resistivity, air in spaces increases it (Omatsola *et al.*, 1981). The use of the electrical resistivity tomography technique (dipole-dipole array) in electrical prospecting has become common. In terms of logistics in the field, it is one of the most convenient techniques, especially for large spacing. The current and potential electrode spacing in a dipole-dipole array is the same, a , and the spacing between them is an integral multiple of a , na . The apparent resistivity is thus

given by:
$$\frac{\rho}{l} \pi a n(n+1)(n+2)$$

The dipole-dipole array is used to measure the curvature of the potential field and is most sensitive to resistivity changes between the electrodes in each electrode pair. A dipole is a pair of oppositely charged electrodes that are so close together that the electric field seems to form a single electric field rather than a field from different electric poles. The dipole-dipole array (Figure 3.1) consists of a current electrode A and B and a potential electrode pair M and N, and it offers a way to plot raw data to get a picture of the cross-section of the earth. It measures the apparent resistivity, which represents a weighted average of the resistivities under the four electrodes used to take the readings. The result is plotted in a pseudo-section. For each measurement, the apparent resistivity data are plotted at the midpoint between the two dipoles and a depth half the distance between the two dipoles.

The values from the investigation were contoured and colorized which represented a rough (and often severely distorted) image of the subsurface. Although it doesn't give an actual image of the ground, the data points resulting from these measurements provide an image of the cross-section of the earth. Two traverses were achieved for each dam location during this research work RTM 1 and RTM 2 for traverse 1 and traverse 2 respectively. Traverse 1 was done closer to the embankment and Traverse 2 along with the downstream of the dam embankment farther away from Traverse 1 which trends NW-SE direction of the dam.

3.0 Results and Discussion

3.1 Residual Magnetic Intensity (RMI)

The residual magnetic intensity map of Apodu dam (Figure 3) shows that the magnetic intensity values ranged from high (127.94 nT) to low (-88.47 nT). Negative anomalies were observed in the area which may be due to the presence of low magnetic rocks (e.g. shale, sandstone, limestone) in the area, that are noted for low magnetic signatures. Removal of the regional magnetic anomaly from the measured anomaly for sheet 223 also gives negative RMI values like that of sheet 202

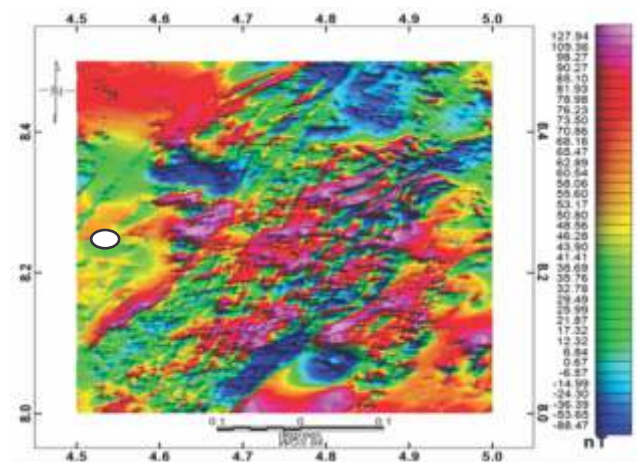


Figure 3: Residual Magnetic Intensity map of sheet 223 (Apodu dam area).

Legend:
○ Apodu dam location

3.2 Reduction to pole (RTP)

Figure 4 shows the RTP map of the Apodu dam area. The RTP map depicts frequency variations present in the magnetized rocks of the area. The RTP places anomalies from the residual magnetic field directly over the magnetic field resulting from causative rocks producing these anomalies. The areas that were displayed as high and low magnetic anomaly zones in RMI maps are now shown as low and high magnetic anomaly zones respectively. Further, contacts between the low and high magnetic susceptible zones have also been enhanced. Various structures such as folds, faults, and rock lithology contacts have also been enhanced. Most of the low magnetic signatures emanate from rocks that have fewer magnetic minerals in them, while high signatures are being produced by rocks that have high magnetic minerals in them. The area of study falls within the basement complex of Nigeria, the basement complex is characterized by rocks of various ages and compositions. The area contains rocks such as migmatite, gneiss, granite, granodiorite, and schist. Most of the low magnetic anomalies come from the meta-sediments while high magnetic susceptibilities are from the competent basement rocks. The patterns that were observed on the RTP map are due to rock deformation especially at the central part of both sheets. The basement rocks have been folded during several phases of deformation and these had allowed the magnetic minerals that are present in such rocks to also reshape themselves in the manner that the host rocks have done. The northwestern part of the RTP map (Figure 4) shows low to moderate magnetic signature variation and has limited structures when compared to the rest of the area. The orientation in the two maps is the NE-SW direction which correlates the structural trends that were measured during the geological field mapping undertaken and have been reported by various authors on the basement complex of Nigeria.

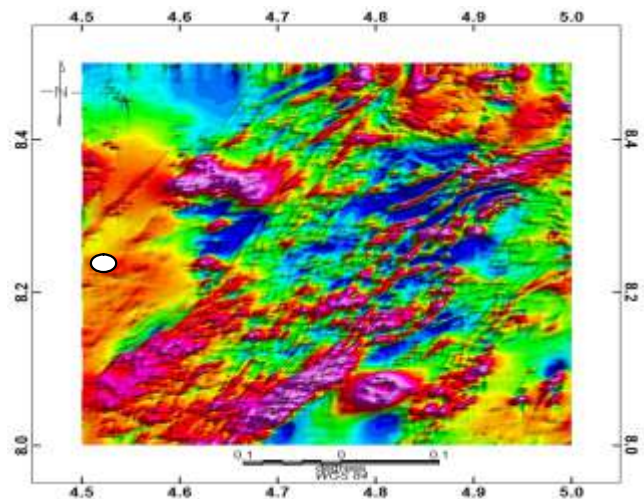


Figure 4: Reduced to pole map of sheet 223 (Apodu dam area)

Legend:
○ Apodu dam location

3.3 First vertical derivative (FVD)

Figure 5 shows the first vertical derivative map of the area of study. The FVD grid was upwardly continued to a hundred meters to subvert the effects of deep source magnetic features

and enhance shallow source magnetic features that are associated with geological structures. The red lines in figure 5 represents lineaments which are structural deformations that are related to geological features and arched zones or even geological contacts. Magnetic minerals are mainly concentrated along or aligned with some structures and lineaments were delineated by observing the abrupt change between the positive and negative magnetic anomalies. This gives a rough idea of the structure and lithologic deformations in the study area.

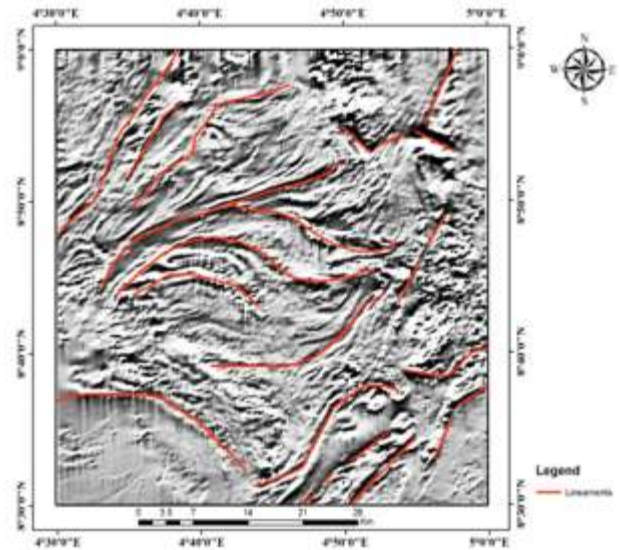


Figure 5: First Vertical Derivative (FVD) map showing lineaments in Apodu dam area

4.4.3 Apodu dam 2-D resistivity Tomography

The first ERT profile was carried out at about 15 m from the center of the dam's embankment along the downstream sides, while the second ERT profile was carried out at the center of the dam's embankment. The two ERT profiles are structured along with SW-NE directions, starting from the dam's embankment towards the spillway (Figure 5). The collected ERT data were inverted using the least-squares method including smoothing of model resistivity to obtain better results from noisy data.



Figure 5: Apodu dam Resistivity Tomography Profiles

The results obtained based on the 2D inversion of the ERT field data were interpreted to characterize the subsurface structure within the investigation depth. The disparity between the measured and computed apparent resistivity values must be reduced for this method to be optimized. This difference is expressed by root mean squared (RMS) error. The ERT field data were collected along traverse 1 and traverse 2 profiles (Figures 5). The data were inverted using *Dipro 4.0* computer software.

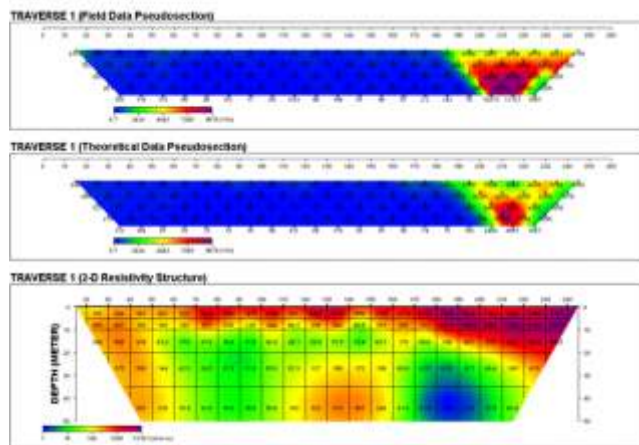


Figure 6: Interpretation of the geoelectrical section of the RTM 1 profile carried out in the upstream/centre of Anoduearthdam embankment

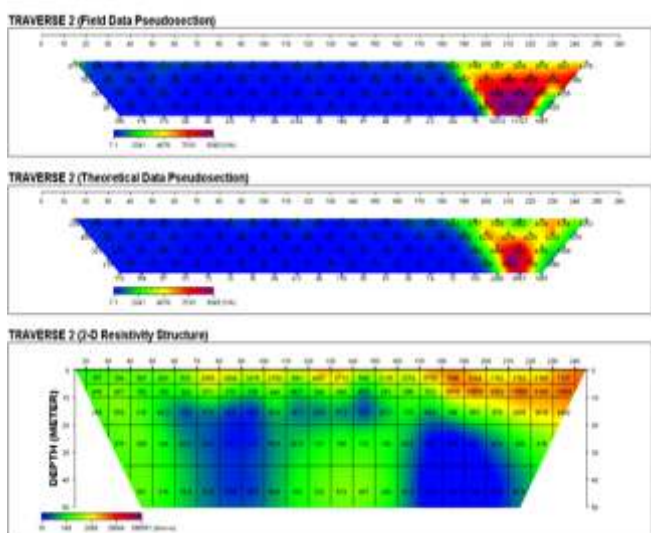


Figure 7: Interpretation of the geoelectrical section of the RTM 2 profile carried out in the downstream of Apoduearthdam embankment

Figures 6 and 7 shows traverse 1 and traverse 2 pseudo-section of Apodu dam established along the dam embankment. It shows both the theoretical, field sections, and resistivity structures. It further shows the cross-section of points RTM 1 and RTM 2 profile of the subsurface up to a depth of 50 m. RTM 1 is along the upstream/center of the dam embankment while RTM 2 is along with the downstream of the dam embankment. The 2-D resistivity image shows three major resistivity zones; very low resistivity indicated by the blue coloration (depicting overburden and/or seepage zones or water-bearing soils), medium-range resistivity indicated by the green to yellow coloration (depicting lateritic soils, weathered basements, and indurated soils that is relatively

impermeable to water), and the high range resistivity indicated by orange to purple coloration (depicting the fresh basement highly competent rocks).

Figure 8 correlates the resistivity of RTM1 and RTM2 of Malete earth embankment. The dam is well compacted at the surface which shows high resistivity values from the surface to about 8m below the surface. RTM1 shows a drop in resistivity values around A, indicating a weakness zone below a depth of 25 m at chainage 170 to 190. RTM2 indicated low resistivity values below 8 m as indicated with B and C, this is observed around chainage 55 to 150 m for zone B and chainage 165 to 218 m. The observed low resistivity indicates a weakness zone that is water-bearing and can be connected in RTM1 and RTM2, suggesting a possible pathway for water. This water pipe way is indicative of a possible seepage zone and adequate measures are expected to be made to arrest the situation.

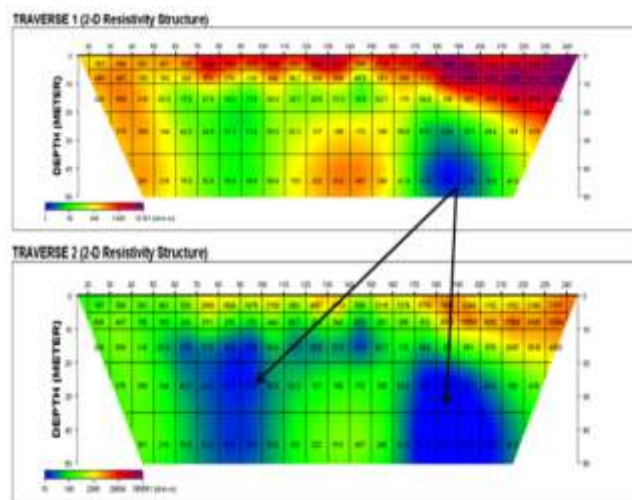


Figure 8: Correlation of RTM1 and RTM2 of Apoduearthdam embankment

4.0 Discussion and Conclusion

The area of study falls within the basement complex of Nigeria. This basement complex has undergone several episodes of deformation (polycyclic) according to Rahman (1984). The patterns of folding and faulting observed on the FVD map (Figures 3) were formed during the various episodes of deformation that the basement rocks have undergone. The basement rocks have been folded during several phases of deformation and this has allowed the magnetic minerals that are present in such rocks to also reshape themselves in the manner that the host rocks have done.

Before recommending an area for dam construction, the area must be tectonically stable, with little or no active faults nearby. This is because the presence of active tectonic structures near the vicinity of a dam will increase significantly the construction cost, technicalities required for its construction and maintenance or may even lead to failure of the dam in the long run which may also affect lives and properties situated around the dam area especially the downstream. As seen in Figure 4, most of the lineaments are concentrated in the mid-part of the area of study and trends in

a NE-SW direction. Shearing is also taking place in the middle part of the area of study. The style of folding and faulting in the area of the study suggests this area could be a shear zone i.e. a place where several shearing is taking place, and as such is not suitable for dam emplacement without proper foundation treatment. This would however make dam construction in such areas more challenging and expensive. The northeastern part of the Apodu dam study area (Figure 4) where the Apodu dam is located, shows little or no sign of faulting and appears to be more stable than the other area of the map. We could therefore deduce from the above that the Apodu dams are located in less structurally active zones and could only likely have a functional failure rather than structural because there are no visible geological structures near the dam area.

Characterization of the Apodu dam subsurface for seepage appraisal using electrical resistivity tomography technique on the other hand revealed that the dam is well compacted at the surface but there are observed low resistivity values indicative of possible occurrences of weakness zones that are water-bearing in some areas of the dam embankment body at depths of around 8m and 25m. The observed low resistivity indicates a weakness zone that is water-bearing and can be connected in RTM1 and RTM2, suggesting a possible pathway for water. This water pipe way is indicative of a possible seepage zone and adequate measures are expected to be made to arrest the situation.

Conclusively, Apodu dam is situated in a geologically stable environment as deduced from the aeromagnetic study but its earth embankment is suspected to possess areas with possible seepages zones as obtained from the electrical resistivity techniques of investigations. There is therefore a need to quickly remedy the dam earth embankment to ensure the longevity of the dam and avert its eventual collapse.

References

- Ako, B.D. (1976). An Integration of Geophysical and Geological Data in Dam Site Investigation-The Case of Opa Dam". *Journal of Mining and Geology*. 13 (1): 1-6.
- Biswas, A.K. and Charttergee, S. (1971). Dam Disasters - An Assessment. *Eng. J. (Canada)*, 54(3): pp. 3-8.
- Cordell, L. and Grauch, V.J.S. (1985) Mapping Basement Magnetization Zones from Aeromagnetic Data in the San Juan Basin, New Mexico. In: Hinze, W.J., Ed., *The Utility of Regional Gravity and Magnetic Anomaly Maps*, Society of Exploration Geophysicists, 181-197.
- Guy, S. and Lund, P.E, (2006). Stability Evaluation of the Medina Dam, the Role of Dams in the 21st Century. 26th Annual USSD Conference San Antonio, Texas, p14
- Hunter, L.E, Powers, M.H and Rose, R.S. (2011). Geophysical evaluation of earthen dam foundations, US army corps of engineers, ISC, p33
- Jayeoba A. and Odumade D., (2015). Geological and Structural Interpretation of Ado-Ekiti Southwest and its Adjoining Areas Using Aeromagnetic Data. AAPG, SEG and SEPM Joint Technical Conference, Oxnard, California, May 3-5, 2015.
- Milligan, P. R. and Gunn, P. J. (1997). Enhancement and presentation of airborne geophysical data. *AGSO Journal of Australian Geology and Geophysics*, 17(2): pp. 64-774.
- Olorunfemi, M.O., Ojo, J.S., Sonuga, F., Ajayi O. and Oladapo, M.I. (2000a) Geoelectrical and Electromagnetic Investigation of the Failed Koza and Nasarawa Earth Dams Around Katsina, Northern Nigeria. *J. Mining Geol.*, 36(1): pp.51 - 65.
- Omatsola, M.E. and Adegoke, O.S. (1981) Tectonic Evolution and Cretaceous Stratigraphy of the Dahomey Basin. *Journal of Mining and Geology*, 18, 130-137.
- Rahaman, M.A. (1998). Recent Advances in the study of the Basement Complex of Nigeria: Precambrian Geology of Nigeria. *Geological Survey of Nigeria*. pp. 11-14.